ISSN 0021-3640, JETP Letters, 2019, Vol. 109, No. 9, pp. 578–583. © Pleiades Publishing, Inc., 2019.
Russian Text © The Author(s), 2019, published in Pis'ma v Zhurnal Eksperimental'noi i Teoreticheskoi Fiziki, 2019, Vol. 109, No. 9, pp. 598–604.

OPTICS
AND LASER PHYSICS

Stimulated Low-Frequency Scattering of Light in an Aqueous Suspension of the Tobacco Mosaic Virus

M. V. Arkhipenko[a], A. F. Bunkin[b], M. A. Davydov[b, *], O. V. Karpova[a], V. B. Oshurko[b], S. M. Pershin[b], V. N. Streltsov[b], and A. N. Fedorov[b]

[a] *Faculty of Biology, Moscow State University, Moscow, 119991 Russia*
[b] *Prokhorov General Physics Institute, Russian Academy of Sciences, Moscow, 119991 Russia*
**e-mail: sbs_michail@mail.ru*

Received March 18, 2019; revised March 28, 2019; accepted March 29, 2019

Stimulated low-frequency scattering of light by aqueous suspensions of the tobacco mosaic virus with the scattering frequency depending on the concentration of the virus is observed for the first time. For concentrations of ~1×10^{12} and ~2×10^{12} cm^{-3}, the Stokes components of scattered light are shifted by ~43.99 and ~31.08 GHz, respectively. At the same time, the competing process of stimulated Brillouin scattering in these heterogeneous media is suppressed. The theory of stimulated emission resulting from normal-mode vibrations of solvent-molecule-loaded cylindrical nanoparticles driven by ponderomotive forces in the field of two copropagating pump electromagnetic waves is developed for the first time. The theoretically estimated frequency shift of the Stokes component is ~50 GHz, which agrees with the experimental result. It remains unclear why a decrease in the thickness of the liquid layer with a simultaneous increase in concentration selectively favors a decrease in the frequency of coherent normal-mode vibrations of the virus participating in stimulated low-frequency scattering.

DOI: 10.1134/S0021364019090066

INTRODUCTION

The investigation of nonlinear optical phenomena in liquid suspensions of nanoparticles allows one to efficiently apply the methods of nonlinear optics for studying biological objects (blood samples, virus suspensions) and offers the possibility of creating high-efficiency sources of terahertz electromagnetic radiation generated in liquid suspensions owing to the coherent excitation of pulsations of dipolar nanoparticles driven by ponderomotive forces induced in a laser electromagnetic field.

In a number of recent studies, nonlinear optical properties of liquid suspensions of nanoparticles were investigated by stimulated scattering. The processes of stimulated scattering in aqueous suspensions of gold and silver nanoparticles were studied in [1], and stimulated low-frequency scattering (SLFS) in an aqueous suspension of gold nanorods caused by the interaction of laser radiation with acoustic modes of nanoparticles was observed in [2]. In particular, a high efficiency of conversion into SLFS radiation was noted. Similar scattering processes in aqueous suspensions of polystyrene nanospheres (particle diameter 70 nm) and suspensions of cauliflower mosaic viruses were observed by us in [3–5]. Taking into account the unambiguous relationship between the normal-mode acoustic frequencies of viruses and their morphology, SLFS can be used for their identification.

Here, we investigate the behavior of SLFS in aqueous suspensions of the tobacco mosaic virus upon the variation of the virus concentration in the liquid.

OBJECTS UNDER STUDY AND EXPERIMENTAL SETUP

We investigated the aqueous suspensions of the tobacco mosaic virus [6] with concentrations of ~0.5×10^{12}, ~1.0×10^{12}, and ~2.0×10^{12} cm^{-3}. The tobacco mosaic virus represents a ribonucleic acid macromolecule in a protein shell [6]. In the first approximation, the virus may be considered as a 300-nm-long elastic rod with a diameter of 18 nm. The suspensions were poured into identical quartz cells.

The experimental layout is shown in Fig. 1. Second harmonic radiation from a single-frequency Nd:YAG laser (wavelength $\lambda = 532$ nm, linewidth $\Delta\nu \sim 0.005$ cm^{-1}, pulse duration $t \sim 10$ ns, pulse energy up to $E_{max} = 40$ mJ, pulse energy spread is ~5–7%) is focused by a lens (Lens 1, $f = 30$ mm) into the middle of the cell. Radiation emitted owing to stimulated scattering in the cell is directed by a wedge glass plate (Beam splitter) and a mirror (Mirror 2) to Fabry–Perot interferometers (Fabry–Perot 1, 2). After inter-

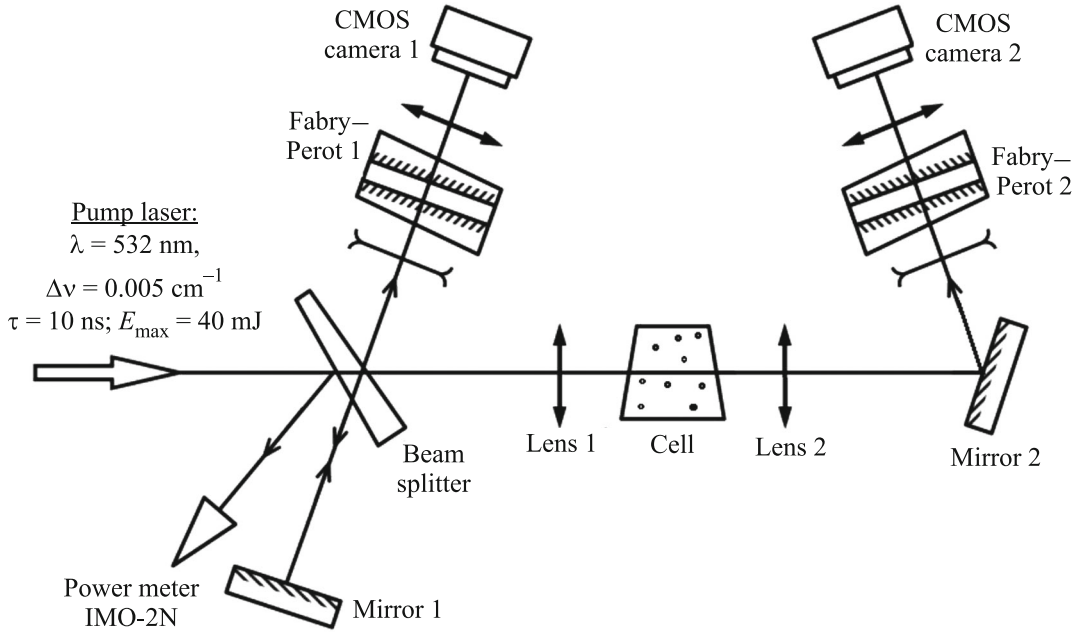

Fig. 1. Layout of the experiment. Beam splitter: a wedge-shaped plate of K-8 glass; Mirror 1, Mirror 2: beam steering mirrors; Lens 1, Lens 2: confocal lenses (f = 30 mm); Cell: quartz cell with the suspension under study; Fabry–Perot 1, Fabry–Perot 2: Fabry–Perot interferometers with focusing optics (the free spectral range of both interferometers is 2.5 cm^{-1}); CMOS 1, CMOS 2: CMOS cameras; Power meter IMO-2N: laser pulse energy meter.

ferometers, the optical signal is recorded by CMOS cameras (CMOS 1, 2) and processed by a computer using LABVIEW software. The laser pulse energy was measured by an IMO-2N calorimeter. The setup configuration was the same for the whole measurement round. Measurements were carried out at room temperature.

EXPERIMENTAL RESULTS AND DISCUSSION

The measurement results are shown in Figs. 2a–2d. The spectrum of radiation scattered by a tobacco mosaic virus suspension with a concentration of ~0.5 × 10^{12} cm^{-3} (Fig. 2a) features only the stimulated Brillouin scattering (SBS) line (backward SBS with a Stokes shift of Δν ~ 0.24 cm^{-1}). An increase in the virus concentration to ~1.0 × 10^{12} cm^{-3} (Fig. 2b) leads to the suppression of SBS from the suspension (previously, we already observed the concentration-dependent suppression of SBS in aqueous suspensions of polystyrene nanospheres [3]). SLFS was observed for a laser pulse energy of ~20 mJ. We note that SLFS radiation propagated in both forward and backward directions. This fact, along with the presence of a spectral line with a frequency shift of Δν ~ 1.47 cm^{-1} (~43.99 GHz), represents the key and characteristic difference from SBS (Figs. 2b, 2d). For the virus concentration of ~2.0 × 10^{12} cm^{-3}, SBS was not observed either, and the SLFS threshold increased to ~30 mJ. It was also found that a reduction in the spacing between the virus particles with increasing concentration manifests itself in the selective decrease of acoustic losses at another eigenfrequency of nanoparticles and the excitation of coherent vibrations with a shift of Δν ~ 1.039 cm^{-1} (~31.08 GHz, see Fig. 2c).

Thus, we observe concentration-dependent competition between the onset of SBS and SLFS in aqueous suspensions of the tobacco mosaic virus. For a virus concentration of ~0.5 × 10^{12} cm^{-3}, the SBS process takes place, while SLFS does not occur up to pulse energies corresponding to optical breakdown in the medium (~35 mJ). With a factor of 2 increase in the virus concentration (to ~1.0 × 10^{12} cm^{-3}), the situation changes dramatically: SBS becomes suppressed, and an SLFS line with a frequency shift of Δν ~ 1.47 cm^{-1} (~43.99 GHz) appears in the spectrum of both forward- and backward-propagating radiation. Upon a further twofold increase in the virus concentration (to ~2.0 × 10^{12} cm^{-3}), SLFS develops at another vibration mode with a frequency shift of Δν ~ 1.039 cm^{-1} (~31.08 GHz).

These measurements demonstrate that, under the described experimental conditions, the tobacco mosaic virus has two SLFS-active modes with frequencies of ~43.99 and ~31.08 GHz whose excitation threshold depends on the concentration of nanoparticles.

The physical parameters of a virus particle suspension do not change significantly as the virus concen-

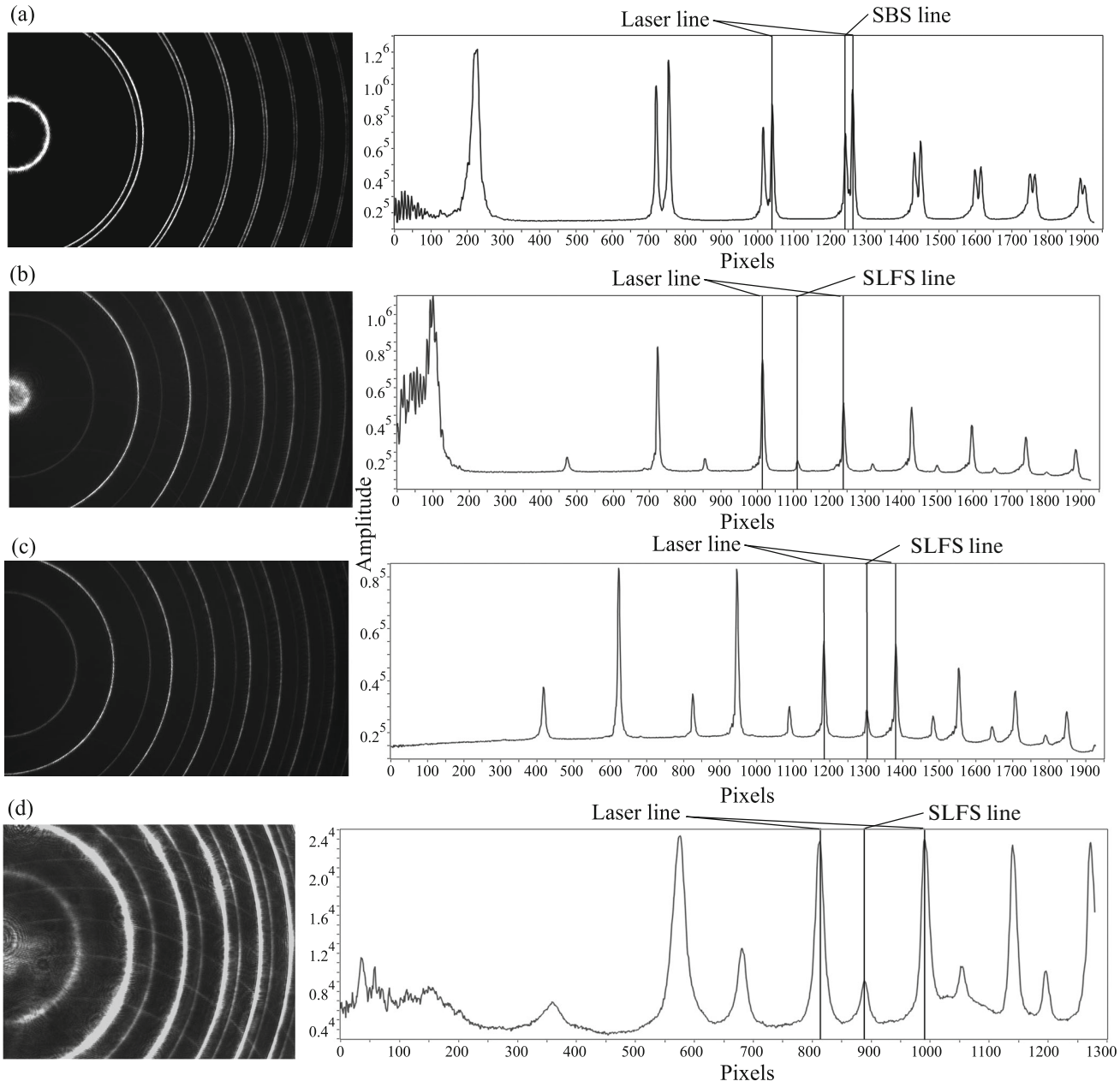

Fig. 2. (a) Spectrum of backward SBS for a concentration of the tobacco mosaic virus of ~0.5×10^{12} cm^{-3}; the frequency shift is $\Delta\nu \sim 0.241$ cm^{-1}. (b) Spectrum of backward SLFS for a concentration of the tobacco mosaic virus of ~1.0×10^{12} cm^{-3}; the frequency shift is $\Delta\nu \sim 1.47$ cm^{-1} (~43.99 GHz). (c) Spectrum of backward SLFS for a concentration of the tobacco mosaic virus of ~2.0×10^{12} cm^{-3}; the frequency shift is $\Delta\nu \sim 1.039$ cm^{-1} (~31.08 GHz). (d) Spectrum of forward SLFS for a concentration of the tobacco mosaic virus of ~1.0×10^{12} cm^{-3}; the frequency shift is $\Delta\nu \sim 1.47$ cm^{-1} (~43.99 GHz). The positions of the laser, SBS, and SLFS lines are labeled in the densitograms by vertical dashes.

tration varies from ~0.5×10^{12} to ~2.0×10^{12} cm^{-3}. For example, the average distance between the particles changes from ~1.2 to ~0.8 μm, which is much greater than the size of the tobacco mosaic virus, and the viscosity of the buffer solution also does not change significantly: simple estimates indicate that the viscosity of the investigated solutions varies in the range of 1.001–1.0037 cP.

THEORY

In this section, we analyze the possibility of stimulated emission that results from the excitation of vibrational eigenmodes of suspended particles in the field of two electromagnetic waves frequency-shifted by some value $\Delta\omega$ (Stokes shift) and copropagating in a liquid containing suspended solid particulates whose refractive index deviates sufficiently from that of the liquid.

We will consider a situation typical of bacterial suspensions (such as the tobacco mosaic virus), in which the transverse dimensions of solid particulates (~18.0 nm) are small compared to their longitudinal dimensions (~300 nm) and the wavelength of the incident laser radiation. At the same time, the wavelengths of induced acoustic vibrations can be less than or comparable to these sizes.

The mechanism of SLFS differs from the mechanism of conventional stimulated Raman scattering (SRS) in that stimulated emission occurs owing to acoustic motions of nanoobjects, which can be excited in a different way than the conventional dipole excitation of vibrational transitions in molecules. For example, in the case of a virus, acoustic vibrations can be excited, first, by ponderomotive forces arising under the action of light waves. Second, much stronger is the direct action of the fields on charges inevitably present at the protein surface owing to the electrolytic dissociation of amino acids in an aqueous environment. Note that these acoustic excitations are fundamentally different from those involved in SBS already because of the fact that they are localized within a nanoobject (virus) and described in a completely different way. As the first approximation, here we consider only the ponderomotive mechanism.

In this context, let us consider the model of infinitely long identically oriented dielectric cylinders of radius R with a dielectric constant ε immersed in a liquid characterized by a density ρ_0, a sound velocity V_S, and a polarizability α_0 corresponding to a dielectric constant ε_0. The suspension is subjected to a fixed field $\mathbf{E}$ formed by two pump waves:

$$\mathbf{E} = \frac{1}{2}\mathbf{E}_0 e^{i(\omega t - kz)} + \frac{1}{2}\mathbf{E}_s e^{i((\omega-\Delta\omega)t-(k-\Delta k)z)} + \text{c.c.} \quad (1)$$

The "reference" wave $\mathbf{E}_0$ and "Stokes" wave $\mathbf{E}_s$ are plane TM-polarized waves; i.e., the magnetic-field vectors $\mathbf{H}_0$ and $\mathbf{H}_s$ are parallel to and the direction z of the wave propagation is perpendicular to the cylinder axis, respectively.

The ponderomotive force $\mathbf{j}_{p.em}$ acting on a unit area of the cylinder surface equals

$$\mathbf{j}_{p.em} = (\langle \mathbf{P} \rangle \cdot \mathbf{n}[\mathbf{E}]. \quad (2)$$

Here, $\langle \mathbf{P} \rangle$ is the average polarizability of the suspension, determined by the polarizability of the particulates and the solvent; $\mathbf{n}$ is the unit vector normal to the cylinder surface, and $[\mathbf{E}]$ is the discontinuity of the normal component of the field at the surface of the cylindrical nanoparticles.

Let us assume that the discontinuity $\Delta\varepsilon = \varepsilon - \varepsilon_0$ of the dielectric constant at the surface is small [7]:

$$\Delta\varepsilon/\varepsilon < 1. \quad (3)$$

This means that the same condition is valid for the polarizability $\Delta\alpha = \alpha - \alpha_0$ (i.e., $\Delta\alpha/\alpha < 1$), and, using the continuity of the normal component of the electric displacement vector, we obtain with sufficient accuracy

$$f_{p.em} = \alpha_0 \frac{\Delta\varepsilon}{\varepsilon}\mathbf{E}^2 \cos^2\theta. \quad (4)$$

Then, without loss of generality, $\mathbf{E}$ is determined by Eq. (1), and θ is the angle between the local vector $\mathbf{n}$ and the constant vector $\mathbf{E}$.

The component that contributes to stimulated emission equals

$$f_{p.em} = \frac{1}{8}\alpha_0 \frac{\Delta\varepsilon}{\varepsilon} E_0 E_S^* (1 + \cos 2\theta) e^{i\Delta\omega t} + \text{c.c.} \quad (5)$$

This situation is physically equivalent to the case of the generation of the Stokes component of SLFS in a suspension of the tobacco mosaic virus, which results from parametric interaction between the pump and Stokes waves. The insignificant differences between the nanoparticle dielectric constants and, correspondingly, their polarizabilities, in the liquid may be the parameter that determines the threshold of SLFS in a suspension of the tobacco mosaic virus.

The ponderomotive force given by Eq. (5) will excite harmonic acoustic vibrations in the cylindrical nanoparticle and the liquid matrix. Owing to the linearity of the boundary conditions (see below), the total acoustic field in the medium will contain, according to Eq. (5), a radially symmetric component and the field of the second azimuthal harmonic ~$\cos 2\theta$.

Let us consider the acoustic field of a cylindrical nanoparticle. In the framework of elasticity theory, we have the following equation for the acoustic displacement vector $\mathbf{u}$:

$$\frac{\partial^2 \mathbf{u}}{\partial t^2} = C_t^2 \Delta\mathbf{u} + (C_l^2 - C_t^2)\text{graddiv}\mathbf{u}. \quad (6)$$

Here, C_l and C_t are the longitudinal and transverse sound velocities, respectively, in the cylindrical nanoparticle. For a radially symmetric harmonic wave u_r with a frequency $\Omega = \Delta\omega$ we obtain, after the usual substitution of variables, the equation

$$\frac{\partial^2 u_r}{\partial x^2} + \frac{1}{x}\frac{du_r}{dx} + \left(1 - \frac{v^2}{x^2}\right)u_r = 0, \quad (7)$$

where $x = k_l r$, $k_l = \dfrac{\Omega}{C_l}$, and

$$V^2 = \frac{1}{2}\frac{C_l^2 - C_t^2}{C_t^2}.$$

The solution of Eq. (7) that remains finite at $r = 0$ is

$$u_r = BJ_v(x), \quad (8)$$

where $J_v(x)$ is the Bessel function.

For the harmonic acoustic field of pressure P in the liquid we have, disregarding damping and viscosity, the conventional hydrodynamic equation

$$\frac{1}{r}\frac{\partial}{\partial r}\left(r\frac{\partial P}{\partial r}\right)+\frac{\Omega^2}{V_S^2}P=0, \tag{9}$$

where V_S is the sound velocity in the liquid.

The solution of Eq. (9) satisfying the radiation condition at $r\to\infty$ can be written as

$$P=AH_0^{(2)}(k_0r), \tag{10}$$

where $k_0=\dfrac{\Omega}{V_S}$ and $H_0^{(2)}(k_0r)$ is the Hankel function.

The boundary conditions for sound waves at the surface of a cylindrical nanoparticle are reduced, as usual, to the requirement of continuity of pressure (taking into account the ponderomotive force) and equality of normal velocities. In our case, the boundary conditions lead to a system of equations for the coefficients A and B:

$$\begin{aligned}B\rho\Omega^2\frac{d^2}{dx^2}[x^\nu J_\nu(x)]\Big|_{r=R}&=-AH_0^{(2)}(k_0r)+\frac{1}{8}\alpha_0\frac{\Delta\varepsilon}{\varepsilon}E_0E_S^*,\\ iB\Omega x^\nu J_\nu(x)\Big|_{r=R}&=iA\frac{1}{\rho V_S}\frac{dH_0^{(2)}(x')}{dx'}\Big|_{r=R},\end{aligned} \tag{11}$$

where ρ is the density of the material forming the nanoparticle and $x'=k_0r$.

The change $U(R,t)$ of the cylinder radius caused by deformation can easily be expressed as

$$\begin{aligned}U(R,t)&=\frac{1}{8}\alpha_0\frac{\Delta\varepsilon}{\varepsilon}E_0E_s^*\frac{1}{\rho C_l\Delta\omega}\\ &\times\frac{J_\nu(X)}{J_{\nu-1}(X)+\left(\dfrac{V_S}{C_l}\right)\left(\dfrac{\rho_0}{\rho}\right)J_\nu(x)\dfrac{H_0^{(2)}(X')}{H_0'^{(2)}(X')}}e^{i\Delta\omega t}+\text{c.c.},\end{aligned} \tag{12}$$

where $X=\dfrac{\Delta\omega}{C_l}R$ and $X'=\dfrac{\Delta\omega}{V_S}R$.

Evidently, the second term in the denominator of Eq. (12) determines radiative losses related to the emission of sound by the pulsating cylinder into the solvent liquid and yields the width of the stimulated scattering generation line.

As would be expected, for $\dfrac{V_S}{C_l}$ and $\dfrac{\rho_0}{\rho}<1$, the acoustic displacement $U(R,t)$ has a sharp maximum corresponding to the normal-mode acoustic vibrations of the cylinder and determined by the resonance condition

$$J_\nu'\left(\frac{\Delta\omega}{C_l}R\right)=0. \tag{13}$$

Taking the values of material constants characteristic of a globular protein (Young's modulus of ~0.9 GPa, density of ~980 kg/m^3, Poisson's ratio of ~0.33), we obtain a frequency of $\Delta\nu\sim 50$ GHz, which approximately corresponds to the experimentally observed values of the frequency shift.

Getting ahead of a later discussion, let us briefly consider the second azimuthal harmonic, excited by the component of the ponderomotive force $\sim\cos 2\theta$. It can readily be demonstrated that shear strain determined by the azimuthal component u_θ of the displacement vector does not affect the cross-section area of the cylinder. The radial component $u_r(R,t)$ is given by the following easily derived expression:

$$u_r=\frac{1}{V_S\rho_0\Delta\omega}\frac{dJ_2}{dx'}\cos 2\theta.$$

Therefore, after integration over θ, the cylinder cross-section area also remains unchanged. It will be seen later that, within the approximations made, this fact leads to zero contribution of the second azimuthal harmonic to stimulated emission.

Let us now calculate the scattered radiation field at the Stokes and anti-Stokes frequencies. The generation of TM-polarized wave can be described by the Helmholtz equation for the magnetic field, which reads in polar coordinates as

$$\begin{aligned}&\frac{1}{r}\frac{\partial}{\partial r}\left(r\frac{\partial\mathbf{H}}{\partial r}\right)+\frac{1}{r^2}\frac{\partial^2\mathbf{H}}{\partial\theta^2}+k^2\mathbf{H}\\ &=-k^2\Delta\varepsilon\mathbf{H}[\theta(r)-\theta(r-R(t)].\end{aligned} \tag{14}$$

Here, k is the wave vector of the scattered wave, $\theta(r)$ is the Heaviside step function, and θ is the azimuthal angle. The right-hand side in Eq. (14) can be designated $\psi(\mathbf{r})$ and considered as the source. The solution of Eq. (14) in polar coordinates is written as a convolution, which leads in the general case to an integral equation:

$$H=\int_S^B G_2(r,r',\theta,\theta')\psi(r',\theta)r'dr'd\theta'. \tag{15}$$

The integral is taken over the cylinder cross section. Here, G_2 is two-dimensional Green's function of the Helmholtz equation:

$$G_2=\frac{i}{4}\sum_{-\infty}^{\infty}H_n^{(2)}(kr)J_n(kr')e^{in(\theta-\theta')}, \tag{16}$$

where $H_n^{(2)}(kr)$ is the Hankel function. The value of the wave vector k will be determined below.

In the case under study $kR<1$, and only the term with $n=0$ should be retained in the sum in Eq. (16). Then, as we will show, integration in Eq. (15) is reduced under certain approximations to the calculation of the cross-sectional area of the cylinder nanoparticle taking into account the acoustic deformation of the latter. This justifies the earlier statement about the second harmonic of the ponderomotive force.

The acoustic displacement $U(R,t)$ of the cylinder surface is small ($\frac{U(R,t)}{R} < 1$), and it is convenient to expand the difference of the Heaviside functions in a formal series:

$$\theta(r) - \theta(r - R - U(R,t)) \approx [\theta(r) - \theta(r - R)] + \delta(r - R)U(R,t). \quad (17)$$

In the Born approximation (see Eq. (3)), the source field H in Eq. (16) is considered fixed and equal to the magnetic field of the reference component of the incident wave:

$$H = \frac{1}{2} H_0 e^{i(\omega t - kz)} + \text{c.c.} \quad (18)$$

Evidently, emission at the Stokes and anti-Stokes frequencies will be determined by the first and second terms in Eq. (15), respectively. The wave vector k of Green's function in Eq. (16) equals

$$k = \frac{\omega \pm \Delta\omega}{C}\sqrt{\varepsilon_0}.$$

Substituting expressions (17) and (18) in Eq. (15), we ultimately obtain

$$H(r,t) = -\frac{i\pi}{4}\frac{(\omega \pm \Delta\omega)^2}{C^2}\Delta\varepsilon H_0 H_0^{(2)} \times \left(\left(\frac{\omega \pm \Delta\omega}{C}\right) r\sqrt{\varepsilon_0}\right) RU(R) e^{i(\omega \pm \Delta\omega)t} + \text{c.c.} \quad (19)$$

Here, $U(R)$ is the factor beside the time-dependent exponent in Eq. (12).

Thus, radiation at the anti-Stokes and Stokes frequencies is generated in a liquid suspension of cylindrical nanoparticles. The spectra of emitted radiation have resonant maxima when the shift $\Delta\omega$ between the frequencies of the reference and anti-Stokes or Stokes waves satisfies Eq. (13). The resonance width is determined by the radiative damping of acoustic vibration eigenmodes of elastic cylindrical nanoparticles.

At the end of this section we note that, given a considerable difference in the longitudinal and transverse velocities of sound in solid particulates and the characteristic radii of the scattering cylinders of $R \sim 10^{-6}$ cm, the lowest resonant frequencies $\Delta\omega$ calculated by Eq. (13) lie in the range near the frequency of $\Delta\nu \sim 50$ GHz, which roughly corresponds to the experimentally observed ones.

CONCLUSIONS

In summary, we have for the first time carried out experiments on the detection of SLFS in aqueous suspensions of the tobacco mosaic virus with different concentrations of suspended particles. We have observed the suppression of SBS with increasing concentration and established the existence of two characteristic eigenmode frequencies of cylindrical nanoparticles of the virus (~31.08 and ~43.99 GHz), which are present in the spectrum of SLFS for the virus concentrations of ~2.0×10^{12} and ~1.0×10^{12} cm^{-3}, respectively.

We have suggested a theory of the ponderomotive excitation of low-frequency scattering in the field of two electromagnetic waves driving the vibrations of cylindrical nanoparticles suspended in a liquid. The ponderomotive effect depends on the dielectric and acoustic parameters of the liquid and solid fractions of the suspension. Numerical estimates of the corresponding vibration frequencies have demonstrated good agreement between the calculated and experimentally determined egeinmode frequencies of cylindrical nanoparticles. In the context of the suggested approach, we mention here the possibility of the selective exposure of viruses to microwave radiation at the frequencies of the detected resonances, which may lead to the emergence of new biotechnologies.

Note that the anti-Stokes component of scattered radiation was not observed in the experiments described above, because the generation of this component is determined either by the parametric conversion of the Stokes component in the field of the pump wave or by the direct amplification of spontaneously emitted thermal radiation at a given frequency in the fixed pump wave field. Anyhow, the anti-Stokes component will have a significantly lower intensity than the Stokes one.

This work is supported in part by the Russian Foundation for Basic Research (project nos. 18-52-16016, 18-52-00038, 19-02-00013) and the Ministry of Science and Education (project no. 3.6634.2017/6.7).

REFERENCES

1. N. V. Tcherniega, K. I. Zemskov, V. V. Savranskii, A. D. Kudryavtseva, A. Yu. Olenin, and G. V. Lisichkin, Opt. Lett. **38**, 824 (2013).
2. J. Shi, H. Wu, J. Liu, Sh. Li, and X. He, Sci. Rep. **2015**, 11964 (2015).
3. A. F. Bunkin, M. A. Davydov, A. N. Fedorov, V. N. Lednev, and S. M. Pershin, Laser Phys. Lett. **16**, 015701 (2019).
4. N. V. Tcherniega, S. M. Pershin, A. F. Bunkin, E. K. Donchenko, O. V. Karpova, A. D. Kudryavtseva, V. N. Lednev, T. V. Mironova, M. A. Shevchenko, M. A. Strokov, and K. I. Zemskov, Laser Phys. Lett. **15**, 095603 (2018).
5. A. F. Bunkin, V. G. Mikhalevich, S. M. Pershin, V. N. Streltsov, and N. V. Tcherniega, Phys. Wave Phenom. **25**, 254 (2017).
6. O. Karpova, N. Nikitin, S. Chirkov, E. Trifonova, A. Sheveleva, E. Lazareva, and J. Atabekov, J. Gen. Virol. **93**, 400 (2012).
7. I. Ermolina, H. Morgana, N. G. Greena, J. J. Milnerb, and Yu. Feldman, Biochim. Biophys. Acta **1622**, 57 (2003).

Translated by M. Skorikov